Thermal and hydrodynamic analysis of a shear-thinning nanofluid in a cylindrical pipe

LABSI Nabila[#1], ALLALOU Nesrine[#2], TOUDJA Nihal[#3], BENKAHLA Youb Khaled[#4]

[#]*Laboratory of Transport Phenomena (team: RSNE), University of Science and Technology Houari Boumediene BP. 32 El Alia, 16111 Bab Ezzouar, Algiers, ALGERIA*

[1]nabilalabsi@yahoo.fr, nlabsi@usthb.dz

[2]nesrineallalou@yahoo.fr

[3]nihale.toudja@gmail.com

[4]youbenkahla@yahoo.fr

***Abstract*— This numerical study focuses on the steady, laminar flow of a non-Newtonian nanofluid inside a pipe maintained at a constant wall temperature. The nanofluid is composed of silver nanoparticles dispersed in a polyethylene melt, whose behavior follows the Carreau-Yasuda rheological model with constant physical and rheological properties. The governing equations of continuity, momentum and energy are solved using an in-house computational code based on the finite volume method. The results indicate that increasing the nanoparticle volume fraction has a beneficial effect on heat transfer but adversely affects the pressure drop since the Fanning friction factor increases. Furthermore, a higher Weissenberg number leads to a reduction in the centerline velocity, thereby decreasing the pressure drop. However, it has a negligible influence on the flow's thermal characteristics.**

***Keywords*— Non-Newtonian nanofluid, silver nanoparticles, Carreau-Yasuda model, Fanning friction factor, Weissenberg number, Nusselt number, finite volume method.**

I. INTRODUCTION

The Carreau-Yasuda rheological model was introduced in order to allow the adjustment of a rheogram over the entire shear range of shear-thinning fluids since the power law model poorly describes the behavior of the fluid at low shear rates. This model well describes the behavior of certain fluids, including polymers. Therefore, the flow of this non-Newtonian fluid through different geometries has been the subject of extensive research. Shamkhi et al. [1] studied numerically, using the PIM meshfree method combined with a characteristic algorithm based on split-A, the flow of a viscous non-Newtonian fluid following the rheological model of Carreau in a cavity. The authors observed a good consistency between the results obtained by the method and the results obtained from the use of the finite volume method for the limiting case of a Newtonian fluid. As revealed by the results, the shear-thinning nature of the fluid strongly affects its flow dynamics inside the cavity. Alloui and Vasseur [2] conducted a numerical analysis of free convection in a vertically oriented cavity containing a non-Newtonian fluid obeying the Carreau-Yasuda rheological model. Neumann-type thermal boundary conditions were applied to the cavity's vertical walls, though the horizontal walls were supposed to be insulated. The authors also studied the same configuration using the power law rheological model and then compared the flow of both fluids. The results indicate a pronounced effect of the fluid's pseudoplasticity on the flow behavior. Khellaf and Laurait [3] considered in their numerical study forced, natural, and mixed convection of a Carreau fluid inside two vertical concentric cylinders; the internal cylinder is heated and in rotation, and the external cylinder is kept cool and motionless. The work examined the impact of the flow index, the Weissenberg and Prandtl numbers, and the radii quotient. The results show that the friction coefficient at the rotating tube and heat exchange in the annular space increase. It has been noted, furthermore, that decreasing the apparent viscosity can produce oscillatory flows, particularly in forced convection by centrifugation. Rousset et al. [4] studied the unsteady stability of Carreau fluid flow over an inclined plane. They analyzed the impact of shear-thinning fluid characteristics on stability determination. Their results show that this fluid exhibits a lower critical Reynolds number than Newtonian fluids. Abbasi et al. [5] undertook a numerical study on the impact of a magnetic field, including the Hall current, on the peristaltic flow of Carreau fluid through a curved conduit, taking into account the Hall Effect. The formulation of the problem relied on lubrication assumptions. The results reveal that, for low values of the pipe's curvature,

ISSN: 2961-6603

the fluid velocity profile becomes asymmetric around the median. Furthermore, increasing the Hall parameter moderates the magnetic influence of the applied field. Lounis et al. [6] numerically examined Carreau-Yasuda fluid thermosolutal convection in an inclined square cavity, considering Soret and Dufour effects. Constant and uniform concentration and temperature were imposed on the active walls while others were insulated and impermeable. They found that increasing the time constant parameter and decreasing the ratio of infinite-to-zero shear rate viscosities led to improved heat and mass transfer for various flow index values. Moreover, the rates of thermal and solutal exchange were enhanced as the inclination angle increased from 0° to 90°.

Convective heat transfer enhancement has been widely investigated in the literature. Indeed, a large number of scientists have carried out numerous numerical and experimental investigations relating to the description of the phenomena, geometry, and physicochemical properties of the fluids. Although more improvement strategies have focused on the geometry of the systems and the physicochemical nature of the convective media, the studies primarily focused on the macroscopic, and occasionally microscopic, aspects of the process. However, since the rise of nanosciences and nanotechnologies in the latter part of the 20th century, convection has evolved to incorporate new enhancement strategies derived from these fields: recent works have been focused on the nanometric level of matter in the convective environment [7-9]. Thus, nanoparticles were introduced into Newtonian or non-Newtonian base fluids. It is worth noting that their addition to fluids could completely change the behavior of the latter. Furthermore, the addition of nanoparticles is beneficial from a thermal point of view, but not from a hydrodynamic point of view.

Some research has been undertaken considering non-Newtonian nanofluids [10-13]. For Carreau-Yasuda nanofluids, Nisar et al. [14] studied numerically the peristaltic mixed convective motion of Carreau-Yasuda nanofluid through a pipe in the presence of slip conditions by considering a modified Darcy's expression for porous space, the Brownian motion, as well as thermophoresis. In addition, the outcomes of first-order chemical reactions and radiation were investigated. They found that the fluid velocity increases for great values of the velocity slip parameter and Weissenberg number, and that heat transfer rate is improved when Brownian motion and thermophoresis are significant. Bilal et al. [15] studied heat transfer in a Carreau-Yasuda-based ternary hybrid nanofluid under a magnetic dipole field across a vertical stretching sheet. The analysis of thermal and velocity fields was carried out considering the combined influence of internal heat generation/sink and Darcy-Forchheimer. The results revealed that the skin friction and the Nusselt number are enhanced by the flow index increase, while higher Darcy-Forchheimer and porosity parameters reduce the velocity profiles. In addition, the hybrid nanofluid revealed higher heat transfer performance over the base fluid across the vertical plate. Akbar et al. [16] investigated the two-dimensional, laminar MHD flow of a Carreau-Yasuda nanofluid over a stretching sheet, driven by surface extension and incorporating quadratic convection. The study also accounted for the effect of variable thermal conductivity and internal heat generation. The analysis reveals that the fluid velocity decreases with increasing magnetic parameter, Brownian motion coefficient and Prandtl number. In contrast, thermal performance improves with higher values of the thermophoretic parameter, variable thermal conductivity and heat generation coefficient. Zid et al. [17] presented a numerical investigation, using the finite difference method, of magnetohydrodynamic free convection involving a shear-thinning SWCNT/water nanofluid, inside a differential heated square porous cavity exposed to a magnetic field. They found that heat and flow behavior are strongly affected by the Carreau-Yasuda the rheological properties and that higher concentrations of nanoparticles raise the fluid’s effective viscosity and improve heat transfer. The study shows moreover that the Lorentz force suppresses the shear-thinning nature of the nanofluid and that the maximum convection performance are obtained for an inclination angle of 30.

In order to contribute to this field of research, and as far as we know, there are few studies that deal with the flow of Carreau-Yasuda nanofluids within pipes, we present this numerical investigation. It is about the analysis of the hydrodynamic and thermal behavior of a Carreau-Yasuda fluid flow within a pipe under the effect of the addition of nanoparticles and the rheological properties (Weissenberg number) variation.

II. Governing Equations and Numerical Approach

The stud y focuses on the steady-state axisymmetric laminar flow of an incompressible non-Newtonian nanofluid within a circular pipe of length L and diameter D. The dilute nanofluid mixture is considered to have uniform physical and rheological properties.

ISSN: 2961-6603

A. Problem statement and nanofluid's thermophysical and rheological properties

The non-Newtonian nanofluid analyzed in the present study consists of a non-Newtonian liquid obeying the rheological model of Carreau-Yasuda, containing suspended nanoparticles. In order to approach reality, we consider silver (Ag) as nanoparticles and the polyethylene melt as a base liquid which follow the Carreau-Yasuda constitutive equation; both are in thermal equilibrium locally.

According to Ansari et al. [18], the polyethylene melt behaves like a Carreau-Yasuda fluid. Its physical and rheological properties are given in Table 1 at a temperature of 160 °C.

On the other hand, we evaluate the physical properties of Ag nanoparticles at the considered temperature (160 °C) using curves given by Smith and Fickett [19] showing the dependence of Ag nanoparticles physical properties on temperature (Table 1).

TABLE I
PHYSICAL AND RHEOLOGICAL PROPERTIES OF SILVER NANOPARTICLES (AG) AND POLYETHYLENE MELT AT 160 °C.

	Ag nano-particles [19]	**Polyethylene melt [18]**
Density (kg/m^3)	10420	782.8
Specific heat (J/kg K)	242.95	2250
Thermal conductivity (W/m K)	381.88	0.170
Viscosity (kg/m s)	-	617.230 (η_0)
Carreau power law index, n	-	0.221
Relaxation time, λ (s)	-	17.727
Yasuda exponent, a	-	0.215

In order to analyze the flow within the pipe, it is necessary to know the thermophysical properties of the nanofluid, which are: density, thermal conductivity and viscosity. The density (ρ_{nf}) and specific heat (Cp_{nf}) are given by the following most-used expressions based on the mixture theory given by Pak and Choi [20]:

$$\rho_{nf} = (1-\phi)\rho_f + \phi\rho_p \quad (1)$$

$$(\rho C_P)_{nf} = (1-\phi)(\rho C_P)_f + \phi(\rho C_P)_p \quad (2)$$

ϕ represents the nanoparticle volume fraction, ρ_f and ρ_p are respectively, the base fluid and nanoparticles densities, Cp_f and Cp_p are the base fluid and nanoparticles specific heat, respectively.

The effective thermal conductivity of the nanofluid, k_{nf}, is given by the Maxwell model proposed in 1873 [20-21] assuming spherical particles, such as:

$$k_{nf} = k_f \left[\frac{k_p + 2k_f - 2\phi(k_f - k_p)}{k_p + 2k_f + \phi(k_f - k_p)} \right] \quad (3)$$

k_f and k_p are the base fluid and particles thermal conductivity, respectively.

Regarding the effective viscosity of the nanofluid (μ_{nf}), Einstein was the first to propose in 1906 an expression to calculate this property for nanofluids having spherical solid particles, but his formulation has some limitations. Thus, many researchers suggest most developed formulations, such as Brinkman, who developed in 1952 a modified Einstein's equation and gave the following expression for the use of particle concentration up to 4% [20-21]:

$$\mu_{nf} = \frac{\mu_f}{(1-\phi)^{2.5}} \quad (4)$$

μ_f is the base fluid viscosity.

As noted above, the base fluid follows the Carreau-Yasuda rheological model, for which the effective viscosity η, i.e. μ_f, is defined as follows [22]:

ISSN: 2961-6603

$$\eta = \eta_\infty + (\eta_0 - \eta_\infty)\left\{\left[1 + (\lambda \dot{\gamma})^a\right]^{\frac{n-1}{a}}\right\} \tag{5}$$

η_0 and η_∞ represent the zero-shear-rate viscosity and the infinite-shear-rate viscosity, respectively, λ is the relaxation time or the time parameter, n denotes the Carreau power-law index (n < 1), a is the Yasuda exponent and $\dot{\gamma}$ represents the shear rate. When assuming $\eta_\infty << 0$, the apparent viscosity of equation (5) becomes:

$$\eta = \eta_0\left\{\left[1 + (\lambda \dot{\gamma})^a\right]^{\frac{n-1}{a}}\right\} \tag{6}$$

The dimensionless form of the Carreau-Yasuda effective viscosity as proposed by Bird et al. [23] is given by the following equation:

$$\eta_{eff} = \left[1 + (We\,\dot{\gamma}^*)^a\right]^{\frac{n-1}{a}} \tag{7}$$

Where We represents the Weissenberg number such as: $We = \lambda D/V_0$, and $\dot{\gamma}^*$ the dimensionless shear rate such as: $\dot{\gamma}^{*2} = 2\left\{\left(\frac{\partial V}{\partial R}\right)^2 + \left(\frac{\partial U}{\partial X}\right)^2 + \left(\frac{V}{R}\right)^2\right\} + \left(\frac{\partial U}{\partial R} + \frac{\partial V}{\partial X}\right)^2$

Therefore from Eq. (4) and (7), the dimensionless form of the Carreau-Yasuda nanofluid's effective viscosity is:

$$\eta_{nf} = \frac{\left[1 + (We\,\dot{\gamma}^*)^a\right]^{\frac{n-1}{a}}}{(1-\phi)^{2.5}} \tag{8}$$

B. Governing equations

The dimensionless governing equations (continuity, momentum and energy) are expressed as:

$$\frac{1}{R}\frac{\partial(RV)}{\partial R} + \frac{\partial U}{\partial X} = 0 \tag{9}$$

$$\begin{aligned}&\frac{1}{R}\frac{\partial(R\,V\,V)}{\partial R} + \frac{\partial(U\,V)}{\partial X} = -\frac{\partial P^*}{\partial R} + \frac{1}{Re}\left(\frac{\rho_f}{\rho_{nf}}\right)\left(\frac{\mu_{nf}}{\mu_f}\right)\left[\frac{1}{R}\frac{\partial}{\partial R}\left(\eta_{eff}\,R\frac{\partial V}{\partial R}\right)\right.\\ &\left.+\frac{\partial}{\partial X}\left(\eta_{eff}\frac{\partial V}{\partial X}\right)\right] + \frac{1}{Re}\left(\frac{\rho_f}{\rho_{nf}}\right)\left(\frac{\mu_{nf}}{\mu_f}\right)\left[\frac{V}{R}\frac{\partial}{\partial R}(\eta_{eff}) - \eta_{eff}\frac{V}{R^2} + \frac{\partial}{\partial X}(\eta_{eff})\frac{\partial U}{\partial R} + R\frac{\partial}{\partial R}(\eta_{eff})\frac{\partial}{\partial R}\left(\frac{V}{R}\right)\right]\end{aligned} \tag{10}$$

$$\begin{aligned}&\frac{1}{R}\frac{\partial(R\,V\,U)}{\partial R} + \frac{\partial(U\,U)}{\partial X} = -\frac{\partial P^*}{\partial X} + \frac{1}{Re}\left(\frac{\rho_f}{\rho_{nf}}\right)\left(\frac{\mu_{nf}}{\mu_f}\right)\left[\frac{1}{R}\frac{\partial}{\partial R}\left(\eta_{eff}\,R\frac{\partial U}{\partial R}\right) + \frac{\partial}{\partial X}\left(\eta_{eff}\frac{\partial U}{\partial X}\right)\right]\\ &+\frac{1}{Re}\left(\frac{\rho_f}{\rho_{nf}}\right)\left(\frac{\mu_{nf}}{\mu_f}\right)\left[\frac{\partial}{\partial R}\left(\eta_{eff}\right)\frac{\partial V}{\partial X} + \frac{\partial}{\partial X}\left(\eta_{eff}\right)\frac{\partial U}{\partial X}\right]\end{aligned} \tag{11}$$

$$\frac{1}{R}\frac{\partial(RV\theta)}{\partial R} + \frac{\partial(U\theta)}{\partial X} = \frac{1}{Pr\,Re}\frac{\alpha_{nf}}{\alpha_f}\left[\frac{1}{R}\frac{\partial}{\partial R}\left(R\frac{\partial\theta}{\partial R}\right) + \frac{\partial^2\theta}{\partial X^2}\right] \tag{12}$$

The ratios: $\left(\frac{\rho_f}{\rho_{nf}}\right)$, $\left[\frac{(\rho Cp)_f}{(\rho Cp)_{nf}}\right]$, $\left(\frac{k_{nf}}{k_f}\right)$ and $\left(\frac{\mu_{nf}}{\mu_f}\right)$ are replaced by their expressions of equations (1), (2), (3) and (4), respectively.

ISSN: 2961-6603

The applied boundary conditions include a uniform axial velocity at the inlet (U = 1, V = 0) and no-slip condition imposed along the pipe wall (U = V = 0).

C. Pressure drop

The pressure drop along fluid flow must be carefully evaluated, especially when the fluid exhibits viscous or non-Newtonian characteristics. In this study, it is estimated through the calculation of the Fanning friction factor $(f\,Re)_x$. It consists of the product between the fluid's apparent viscosity at the wall and the wall velocity gradient (wall shear rate), as follows:

$$(f\,Re)_x = 2\left(\eta_{nf}\,\dot{\gamma}^*\right)\Big|_{R=0.5} \tag{13}$$

D. Heat transfer rate

The rate of heat exchange within a configuration is estimated by calculating the Nusselt number. This is a dimensionless number used in heat transfer operations. It represents the ratio between convective and conductive heat transfer across an interface, often between a fluid and a solid. When conduction is the dominant mode of heat transfer, the Nusselt number is typically on the order of one. However, in the presence of convection, heat is mainly transferred through fluid motion, which causes the Nusselt number to increase significantly and tend toward infinity. Thus:

$$Nu = \frac{h\,D}{k_{nf}} \tag{14}$$

In order to estimate heat transfer rate between the pipe wall and the fluid, the following expression for the Nusselt number is used:

$$Nu_x = -\left(\frac{k_{nf}}{k_f}\right)\frac{1}{\theta_m}\frac{\partial\theta}{\partial R}\Big|_{R=0.5} \tag{15}$$

E. Numerical modelling

The elliptic set of partial differential equations (9)-(12) and the associated boundary conditions are numerically resolved via the finite volume method formulated by Patankar [24], which guarantees full conservation of mass and momentum within the computational domain. Thus, the governing equations are reformulated as algebraic expressions in terms of the unknown velocities and pressure at specific grid locations.

An in-house computational code employing the line-by-line solver technique is used to resolve these equations. A non-uniform grid is used, with mesh refinement applied at the inlet and near the pipe wall. The optimal meshing implemented consists of 250x40 nodes in the X and R directions, respectively. Convergence is achieved when the residuals fall below 10^{-5} for velocities and 10^{-6} for pressure. Finally, 10^4 iterations were necessary to reach the solution.

To validate the accuracy of the developed computational code, a limiting case corresponding to Newtonian fluid (n = 1 and/or We = 0) was considered. Thus, the obtained velocity profile and Nusselt number evolution were compared with the results of Min et al. [25]. As shown in Figure 1, the comparison reveals good agreement, with a relative deviation not exceeding 2%.

ISSN: 2961-6603

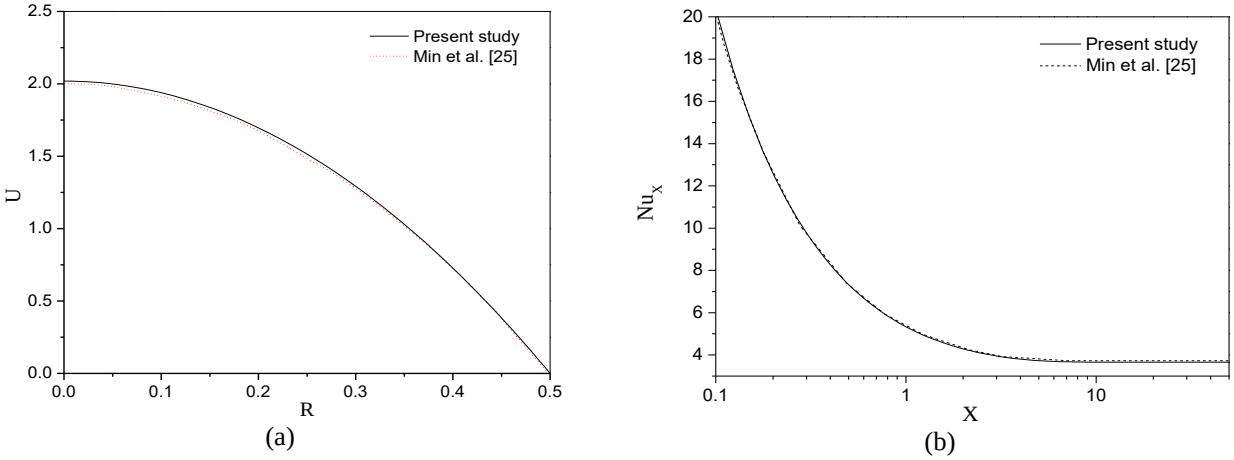

Fig. 1 Velocity profile (a) and Nusselt number axial evolution (b). Pe = Re*Pr = 50, We = 0.

III. Results and Discussion

The objective of this study is to analyze the flow within a pipe, of a shear-thinning nanofluid whose base fluid follows the Carreau-Yasuda rheological constitutive equation. The flow is analyzed under the influence of volume fraction of nanoparticles as well as rheological properties. Thus, the numerical simulations were undertaken for nanoparticles volume fraction $0 \leqslant \phi \leqslant 0.05$ and a Weissenberg number $0 \leqslant We \leqslant 2.20$ regarding the rheological properties of polyethylene melt in Table 1. It t should be noted that the Weissenberg number is a dimensionless number permitting the comparison of viscous and elastic forces of a fluid; it indicates the degree of anisotropy or the orientation generated by the deformation.

All the simulations were obtained for a moderate Peclet number value of 1000 since polyethylene melt has a high Prandtl number and axial diffusion is neglected when the Peclet number exceeds 100 [26]. The literature reveals that the Peclet number values for polymer melt range between 10^3 and 10^6.

A. Hydrodynamic behaviour

In order to analyse the effect of the nanoparticle volume fraction ϕ on pressure drop within the pipe, we present in Figures 2 and 3, the Fanning friction factor $(f\,Re)_x$ axial evolution for different values of ϕ and We, respectively.

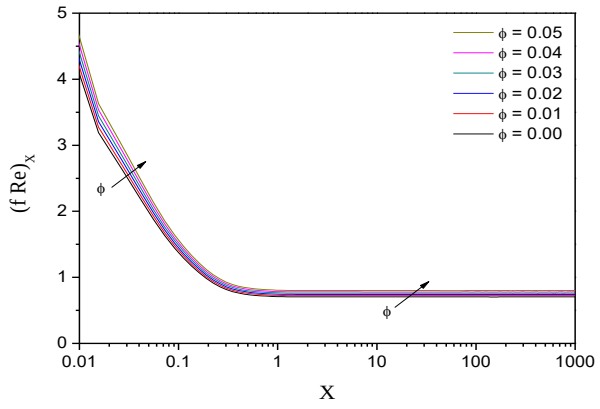

Fig. 2 Fanning friction factor evolution for different values of the nanoparticles volume fraction. Pe = 1000, We = 0.68.

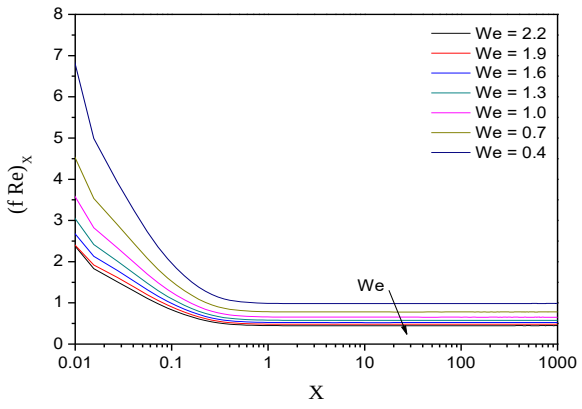

Fig. 3 Fanning friction factor evolution for different values of the Weissenberg number. Pe = 1000, ϕ = 0.04.

We can see that the curves follow the same pattern: a decrease in $(f\,Re)_x$ from the entrance until reaching asymptotic and different values, depending on the nanoparticles volume fraction and the Weissenberg number. This is attributed to the decrease in the wall velocity gradient along the pipe until it reaches a constant value,

ISSN: 2961-6603

corresponding to a fully developed hydrodynamic regime where the velocity profile becomes independent of the axis of the flow, as seen in Figure 3.

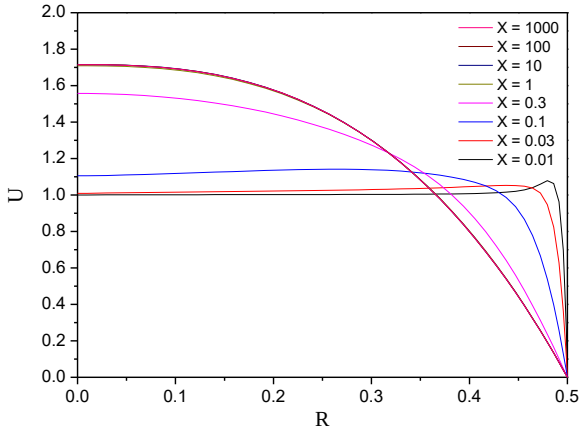

Fig. 4 Velocity profile. Pe = 1000, We = 0.68, ϕ = 0.02.

In the fully developed region (Figure 2), $(f\ Re)_x$ reaches asymptotic values depending on the nanoparticle volume fraction. The impact of incorporating nanoparticles into the base fluid is visible since increasing their volume fraction intensifies $(f\ Re)_x$ throughout the pipe. This influence results from the directly proportional variation in the effective viscosity of the fluid as a function of the nanoparticle volume fraction, according to Eq. (8), and not from the effect of the latter on the velocity gradient at the wall, where the effect is almost non-existent, as seen in Figure 5.

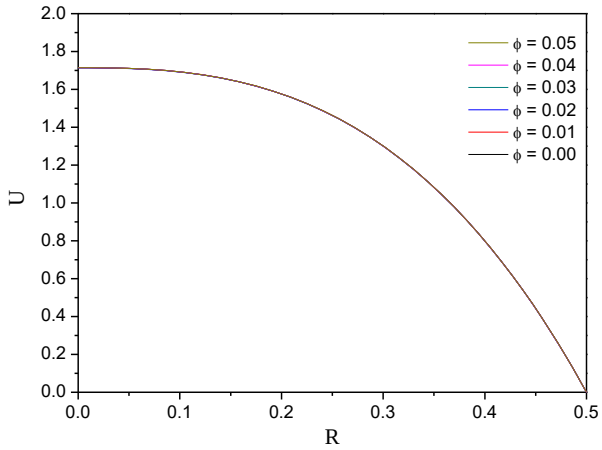

Fig. 5 Velocity profile via the nanoparticle volume fraction in the fully developed region. Pe = 1000, We = 0.68, X = 1000.

Therefore, the presence of nanoparticles has a negative influence since it tends to increase $(f\ Re)_x$ and, consequently, the pressure drop within the pipe. This effect is all the more significant as ϕ is high. This is well represented in Figure 6, which shows the ratio of $(f\ Re)_x$ between the Carreau-Yasuda nanofluid ($\phi \neq 0$) and the base Carreau-Yasuda fluid ($\phi = 0$). Indeed, the pressure drop increases, in comparison to the base fluid, by about 2.5% for ϕ = 0.01 and reaches 14% for ϕ = 0.05.

ISSN: 2961-6603

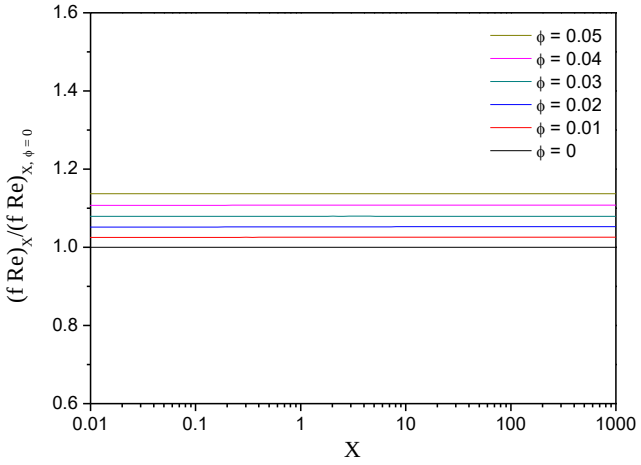

Fig. 6 Fanning friction factor ratio variation via the nanoparticle volume fraction. Pe = 1000, We = 0.68.

Concerning the effect of the Weissenberg number (Figure 3), we observe that the increase in the latter results in a reduction in $(f\ Re)_x$ and a corresponding increase in the fully developed hydrodynamic length. However, Figure 7, which illustrates the velocity profile downstream (X = 1000) according to the Weissenberg number variations, shows that the latter enhanced the wall velocity gradient.

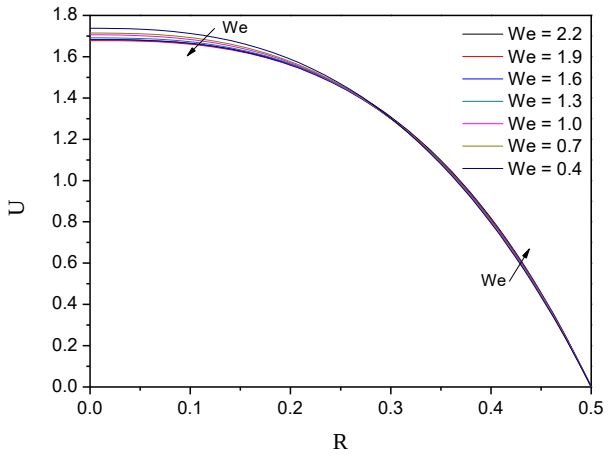

Fig. 7 Velocity profile for different values of the Weissenberg number in the fully developed region. Pe = 1000, ϕ = 0.04, X = 1000.

Thus, it is expected from Eq. (13) that this will have a positive impact on $(f\ Re)_x$, which is not the case. Indeed, although the wall velocity gradient increases, $(f\ Re)_x$ decreases. This can only be due to the fact that it is the dependence of effective viscosity on the Weissenberg number (Eq. (8)) that determines the friction factor's response, according to Eq. (13).

This behavior resembles that found by Khan et al. [27] in their investigation regarding the flow of a Carreau-Yasuda fluid by considering Soret and Dufour effects.

B. Thermal behaviour

Unlike their effect on hydrodynamic behavior, the impact of the nanoparticle volume fraction and the Weissenberg number is almost negligible on heat transfer, as shown in Figures 8 and 9, which illustrate the Nusselt number variation along the pipe as a function of ϕ and We, respectively.

ISSN: 2961-6603

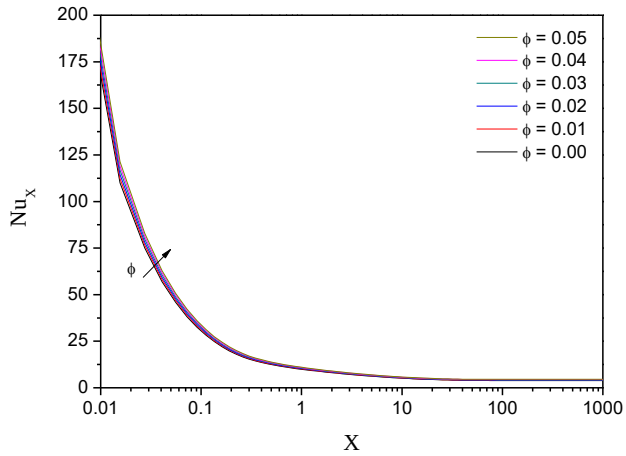

Fig. 8 Nusselt number variation according to the nanoparticle volume fraction. Pe = 1000, We = 0.68.

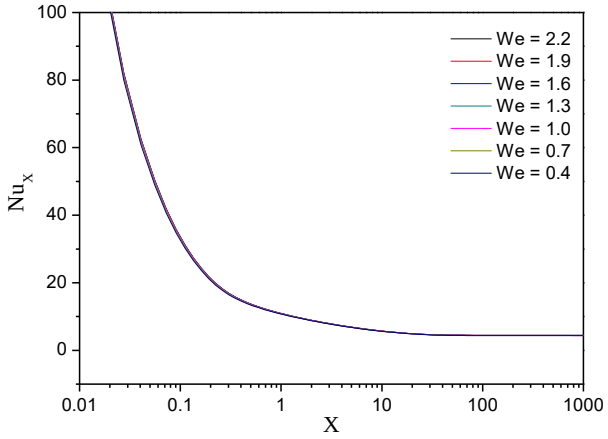

Fig. 9 Nusselt number variation for different values of the Weissenberg number. Pe = 1000, ϕ = 0.04.

Similar to $(f \cdot Re)_x$ evolution, the curves in both figures exhibit the same trend: a decrease in the Nusselt number is observed close to the pipe entrance, attributed to a strong wall temperature gradient, followed by an asymptotic approach to a limiting value. This limiting value depends on the nanoparticle presence and the Weissenberg number, indicating the achievement of the thermal fully developed flow.

As shown in Figure 8, the effect of nanoparticle volume fraction on the Nusselt number, though limited, is noticeable in the inlet region. Actually, in this region, rising nanoparticle concentration enhances heat transfer, reflected by a higher Nusselt number, and reduces the length of the thermally fully developed region. Indeed, literature confirms that nanoparticles significantly improve heat transfer rates because of their high thermal conductivity, which increases the effective thermal conductivity of the nanofluid in comparison to the base fluid.

It can be seen from Figure 10, which present the ratio of Nu_x between the Carreau-Yasuda nanofluid ($\phi \neq 0$) and the base Carreau-Yasuda fluid ($\phi = 0$), an enhancement of approximately 3.05% and 15.8% in heat transfer is observed due to the addition of nanoparticle volume fraction of 0.01 and 0.05, respectively.

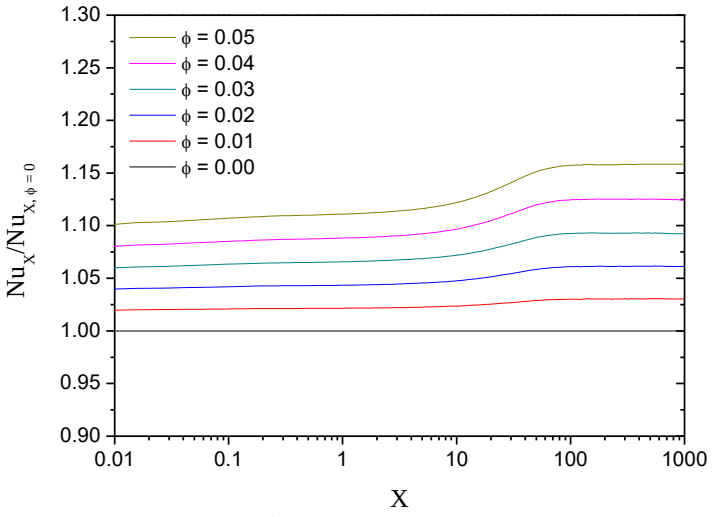

Fig. 10 Nusselt number ratio according to the nanoparticle volume fraction. Pe = 1000, We = 0.68.

In contrast, the impact of the Weissenberg number on Nusselt number variation, as shown in Figure 9, is minimal. This can likely be attributed to the relatively low values of this dimensionless number used in the study. In fact, we tried to respect the data of Table 1 regarding the rheological properties of the fluid.

ISSN: 2961-6603

IV. CONCLUSIONS

This numerical investigation focused on the flow and heat transfer behavior of Ag/Carreau-Yasuda nanofluid within a pipe under the effect of nanoparticle volume fraction and Weissenberg number variations.

The results reveal that the presence and increased volume fraction of nanoparticles contribute to a rise in the Fanning friction factor. Despite the fact that nanoparticles improve heat transfer because of the rise in effective thermal conductivity (as seen in the bibliographical review), their presence intensifies viscous friction within the fluid and thus amplifies the pressure drop, which acts negatively on the flow.

The rise of the Weissenberg number, for its part, results in a decrease in both the centerline velocity and the Fanning friction factor given that the effective viscosity of the nanofluid is directly proportional to the Weissenberg number variation. However, its influence is almost insignificant on heat transfer behavior, through the Nusselt number because of its low values considered in this study. On the other hand, as expected, the incorporation of nanoparticles improves thermal exchange between the wall and the non-Newtonian nanofluid.

ACKNOWLEDGMENT

The authors gratefully acknowledge the support of the General Directorate of Scientific Research and Technological Development (DGRSDT), under the Ministry of Higher Education and Scientific Research of Algeria (MESRS).

REFERENCES

[1] Shamekhi A., Sadeghy K. (2009). Cavity flow simulation of carreau-yasuda non-newtonian fluids using PIM meshfree method. J. Applied Mathematical Modelling. 33: 4131-4145.

[2] Alloui Z., Vasseur P. (2015). Natural convection of Carreau-Yasuda non-newtonian fluids in a vertical cavity heated from the sides. J. Heat Mass Transfer. 84: 912-924.

[3] Khellaf K., Lauriat G. (2000). Numerical study of heat transfer in a non-Newtonian Carreau-fluid between rotating concentric vertical cylinders. J. Non-Newtonian Fluid Mech. 89: 45-61.

[4] Rousset F., Millet S., Botton V., Ben Hadid H. (2007). Temporal stability of Carreau fluid flow down an incline. J. Fluids Eng. 129: 913-920.

[5] Abbasi F.M., Hayat T., Alsaedi A. (2015). Numerical analysis for MHD peristaltic transport of Carreau-Yasuda fluid in a curved channel with hall effects. J. Magnetism and Magnetic Materials. 382: 104-110.

[6] Lounis S., Rebhi R., Hadidi N., Lorenzini G., Menni Y., Ameur H., Che Sidik N.A. (2022). Thermo-solutal convection of Carreau-Yasuda non-Newtonian fluids in inclined square cavities under Dufour and Soret impacts. CFD Letters. 14(3): 96-118.

[7] Çiftçia H., Ersoya B., Evcin A. (2019). Synthesis, characterization and Cr(VI) adsorption properties of modified magnetite nanoparticles. ACTA Physica Polonica A. 132: 564-569. DOI: 10.12693/APhysPolA.132.564

[8] Sözen A., Öztürk A., Özalp M. (2019). Influences of alumina and fly ash nanofluid usage on the performance of recuperator including heat pipe bundle. Int. J. Environ. Sci. Technol.. 16: 5095-5100. DOI: https://doi.org/10.1007/s13762-018-1832-6

[9] Yıldız Ç., Arıcı M., Karabay H. (2019). Effect of inclination angle on natural convection of nanofluids in a U-shaped cavity. Int. J. Environ. Sci. Tech. 16: 5289-5294. DOI: https://doi.org/10.1007/s13762-019-02407-2

[10] Moawed M., El-Maghlany W., Ali R.K., Hamed M. (2014). Forced convection heat transfer inside tube for non-Newtonian fluid flow utilizing nanofluid. Int. J. Applied Sci. and Eng. Res. 3(4): 889-898. DOI: 10.6088/ijaser.030400013

[11] Ouahouah A., Labsi N., Chesneau X., Benkahla Y.K. (2021). Natural convection within a non-uniformly heated cavity partly filled with a shear-thinning nanofluid and partly with air. J. Non-Newtonian Fluid Mech. 289(3): 104-490. DOI: 10.1016/j.jnnfm.2021.104490

[12] Lahlou S., Labsi N., Benkahla Y.K, Boudiaf A., Ouyahia S-E. (2020). Flow of viscoplastic fluids containing hybrid nanoparticles: Extended Buongiorno's model. J. Non-Newtonian Fluid Mech. 281, Article 104308. DOI: https://doi.org/10.1016/j.jnnfm.2020.104308

[13] Toudja N., Labsi N., Benkahla Y.K., Ouyahia S-E., Benzema M. (2022). Thermosolutal mixed convection in a lid-driven irregular hexagon cavity filled with MWCNT–MgO (15–85%)/CMC non-Newtonian hybrid nanofluid. J. Thermal Analy. and Calorim. 147: 855-878. DOI: https://doi.org/10.1007/s10973-020-10288-8

[14] Nisar Z., Hayat T., Alsaedi A., Momani S. (2022). Peristaltic flow of chemically reactive Carreau-Yasuda nanofluid with modified Darcy's expression. Materialstoday Communications. 33, Article 104532. DOI: https://doi.org/10.1016/j.mtcomm.2022.104532

ISSN: 2961-6603

[15] Bilal M., Ullah I., Alam M.M., Shah S.I., Eldin S.M. (2023). Energy transfer in Carreau Yasuda liquid influenced by engine oil with Magnetic dipole using tri-hybrid nanoparticles. Scientific Reports. 13, Article 5432. DOI: https://doi.org/10.1038/s41598-023-32052-2.
[16] Akbar A.A., Awan A.U., Nadeem S., Ahammad N.A., Raza N., Oreijah M., Guedri K., Allahyani S.A. (2024). Heat transfer analysis of Carreau-Yasuda nanofluid flow with variable thermal conductivity and quadratic convection. J. Comp. Design and Eng. 11(1): 99-109. https://doi.org/10.1093/jcde/qwae009
[17] Zid I., Alilat D., Rebhi R., Alliche M., Chamkha A.J., Zeguai S. (2025). MHD natural convection of non-Newtonian Carreau–Yasuda nanofluid in a square porous cavity by Dupuit–Darcy model. https://doi.org/10.1140/epjp/s13360-025-06407-9
[18] Ansari M., Zisis T., Hatzikiriakos S.G., Mitsoulis E. (2012). Capillary flow of low-density polyethylene. Polymer Eng. Sci. 52(3): 649-662. DOI: https://doi.org/10.1002/pen.22130
[19] Smith D.R., Fickett F.R. (1995). Low-temperature properties of Silver. J. Res. Natl. Inst. Stand. Technol. 100: 119-171.
[20] Saini D.K., Agarwal G.D. (2016). Thermo-physical properties of nanofluids - Review. Int. J. Advances Eng. Sci. Tech. 5(1): 39-45.
[21] Fohanno S., Polidori G., Popa C. (2012, March 15). Nanofluides et transfert de chaleur par convection naturelle. Journée Thématique SF. Paris, France.
[22] Steffe J.F. (1992). Rheological methods in food process engineering. 2nd Ed. Freeman Press, USA.
[23] Bird R.B., Armstrong R.C., Hassager O. (1978). Dynamics of Polymeric Liquids, Vol. 1 Fluid Mechanics. 2nd Ed., Wiley and sons, New York.
[24] Patankar S.V. (1980). Numerical heat transfer and fluid flow. Hemisphere, New York.
[25] Min T., Choi H.G., Yoo J.Y., Choi H. (1997). Laminar convective heat transfer of a Bingham plastic in a circular pipe-II. Numerical approach-hydrodynamically developing flow and simultaneously developing flow. Int. J. Heat Mass Trans. 40: 3689-3701.
[26] Nouar C., Benaouda-Zouaoui B., Desaubry C. (2000). Laminar mixed convection in a horizontal annular duct. Case of thermodependent non-Newtonian fluid. Eur. J. Mech. B – Fluids. 19: 423-452.
[27] Khan M.I., Hayat T., Afzal S., Khan M.I., Alsaedi A. (2020). Theoretical and numerical investigation of Carreau–Yasuda fluid flow subject to Soret and Dufour effects. Comp. Meth. Progr. Biomedicine. 186, Article 105145.

NOMENCLATURE

a	Yasuda parameter
Cp	specific heat
D	pipe diameter (m)
h	convective coefficient (W/m² °C)
k	Thermal conductivity (W/m °C)
L	pipe length (m)
n	Carreau flow index
Pe	Peclet number, = Re Pr
Pr	Prandtl number
P*	dimensionless pressure, $= p^* / \rho V_0^2$
p*	pressure (Pa)
r	radial coordinate (m)
R	dimensionless radial coordinate, = r/D
Re	Reynolds number
T	temperature (°C)
T_0	inlet temperature (°C)
T_m	mean temperature (°C)
T_w	wall temperature (°C)
U	dimensionless axial velocity, = V_x/ V_0
V	dimensionless radial velocity, = V_r/ V_0
V_x	axial velocity (m/s)
V_r	radial velocity (m/s)

ISSN: 2961-6603

V_0 inlet velocity (m/s)
x axial coordinate (m)
X dimensionless axial coordinate, = x/D

Greek:
$\dot{\gamma}$ shear rate (s^{-1})
$\dot{\gamma}^*$ dimensionless shear rate, $= \dot{\gamma} D/V_0$
μ viscosity (kg/m s)
ρ fluid's density (kg/m^3)
θ dimensionless temperature, $= \frac{T - T_w}{T_0 - T_w}$
θ_m dimensionless mean temperature, $= \frac{T_m - T_w}{T_0 - T_w}$

Indices :
f fluid
nf nanofluid
p solid particles

ISSN: 2961-6603